Recognition of 16S rRNA by Ribosomal Protein S4 from *Bacillus stearothermophilus*†

Resi B. Gerstner,‡ Yong Pak, and David E. Draper*

Department of Chemistry, The Johns Hopkins University, 3400 North Charles Street, Baltimore, Maryland 21218

Received January 4, 2001; Revised Manuscript Received April 24, 2001

ABSTRACT: Protein S4 is essential for bacterial small ribosomal subunit assembly and recognizes the 5′ domain (∼500 nt) of small subunit rRNA. This study characterizes the thermodynamics of forming the S4−5′ domain rRNA complex from a thermophile, *Bacillus stearothermophilus*, and points out unexpected differences from the homologous *Escherichia coli* complex. Upon incubation of the protein and RNA at temperatures between 35 and 50 °C under ribosome reconstitution conditions [350 mM KCl, 8 mM $MgCl_2$, and 30 mM Tris (pH 7.5)], a complex with an association constant of $\gtrsim 10^9$ M^{-1} was observed, more than an order of magnitude tighter than previously found for the homolgous *E. coli* complex under similar conditions. This high-affinity complex was shown to be stoichiometric, in equilibrium, and formed at rates on the order of magnitude expected for diffusion-controlled reactions ($\sim 10^7$ M^{-1} s^{-1}), though at low temperatures the complex became kinetically trapped. Heterologous binding experiments with *E. coli* S4 and 5′ domain RNA suggest that it is the *B. stearothermophilus* S4, not the rRNA, that is activated by higher temperatures; the *E. coli* S4 is able to bind 5′ domain rRNA equally well at 0 and 37 °C. Tight complex formation requires a low Mg ion concentration (1−2 mM) and is very sensitive to KCl concentration $\{-\partial[\log(K)]/\partial(\log[\mathrm{KCl}]) = 9.3\}$. The protein has an unusually strong nonspecific binding affinity of $3-5 \times 10^6$ M^{-1}, detected as a binding of one or two additional proteins to the target 5′ domain RNA or two to three proteins binding a noncognate 23S rRNA fragment of the approximately same size. This binding is not as sensitive to monovalent ion concentration $\{-\partial[\log(K)]/\partial(\log[\mathrm{KCl}]) = 6.3\}$ as specific binding and does not require Mg ion. These findings are consistent with S4 stabilizing a compact form of the rRNA 5′ domain.

Ribosomal protein S4 is one of the most extensively studied of the 21 small subunit proteins. In early studies of ribosomes, S4 was identified as a protein that bound directly to 16S rRNA (*1*), was essential for in vitro assembly of 30S subunits (*2*, *3*), and was the first protein to bind 16S rRNA during ribosome assembly in vivo (*4*). S4 was found to protect an unusually large region of 16S rRNA from nuclease digestion (*5*, *6*), ∼500 nt termed the 5′ domain, though footprinting experiments seemed to narrow the actual contact region to a "five-helix junction" within which the 5′ and 3′ ends of the protected domain are base paired (*7*, *8*). Recently determined crystal structures of the intact 30S subunit confirm that S4 binds only the five-helix junction (Figure 1; *9*, *10*). The central position of S4 in ribosome assembly and its interaction with a large domain of the rRNA have suggested that S4 contributes to ribosome assembly by organizing the rRNA into a structure competent to bind additional proteins (*11*).

To understand the consequences of S4 binding for rRNA folding and ribosome assembly, it is essential to characterize the thermodynamics of S4−rRNA interactions. A few studies measured binding affinities of *Escherichia coli* S4 protein for 16S rRNA and its fragments under ribosome reconstitution conditions (*12*−*14*), but the marginal stability of *E. coli* S4, which is significantly unfolded at 37 °C (*15*), limited both thermodynamic and structural studies. To obtain a more suitable system for RNA binding and ribosome assembly studies, we have characterized an S4 homologue from the thermophile *Bacillus stearothermophilus* (Bst).[1] Bst S4 is highly homologous to the *E. coli* protein and readily assembles into ribosome subunits with *E. coli* 16S rRNA (*16*, *17*). It is also stable up to ∼70 °C (unpublished observations) and can be purified without strongly denaturing conditions. The structure of a large C-terminal fragment of the protein has been determined by NMR and crystallography (*18*−*20*); the 41 missing N-terminal residues are completely disordered by several NMR criteria (*21*). In the work presented here, we show that Bst S4 binds the 5′ domain of Bst 16S rRNA with an unexpectedly high affinity, more than an order of magnitude stronger than previously found for the homologous *E. coli* S4−rRNA complex. Binding is strongly dependent on K^+ and Mg^{2+} concentrations, as expected for a basic protein stabilizing a compact RNA conformation. We unexpectedly found that Bst S4 binding kinetics are extremely temperature dependent, a feature not observed with the *E. coli* protein and relevant to thermophile ribosome assembly.

† This work was supported by NIH Grant GM56968.

* Corresponding author. Telephone: (410) 516-7448. Fax: (410) 516-8420. E-mail: draper@jhunix.hcf.jhu.edu.

‡ Present address: Department of Oncology MS 60, Genentech, Inc., 1 DNA Way, South San Francisco, CA 94080.

[1] Abbreviations: Bst, *B. stearothermophilus*; Eco, *E. coli*.

10.1021/bi010026i CCC: $20.00
Published on Web 05/24/2001

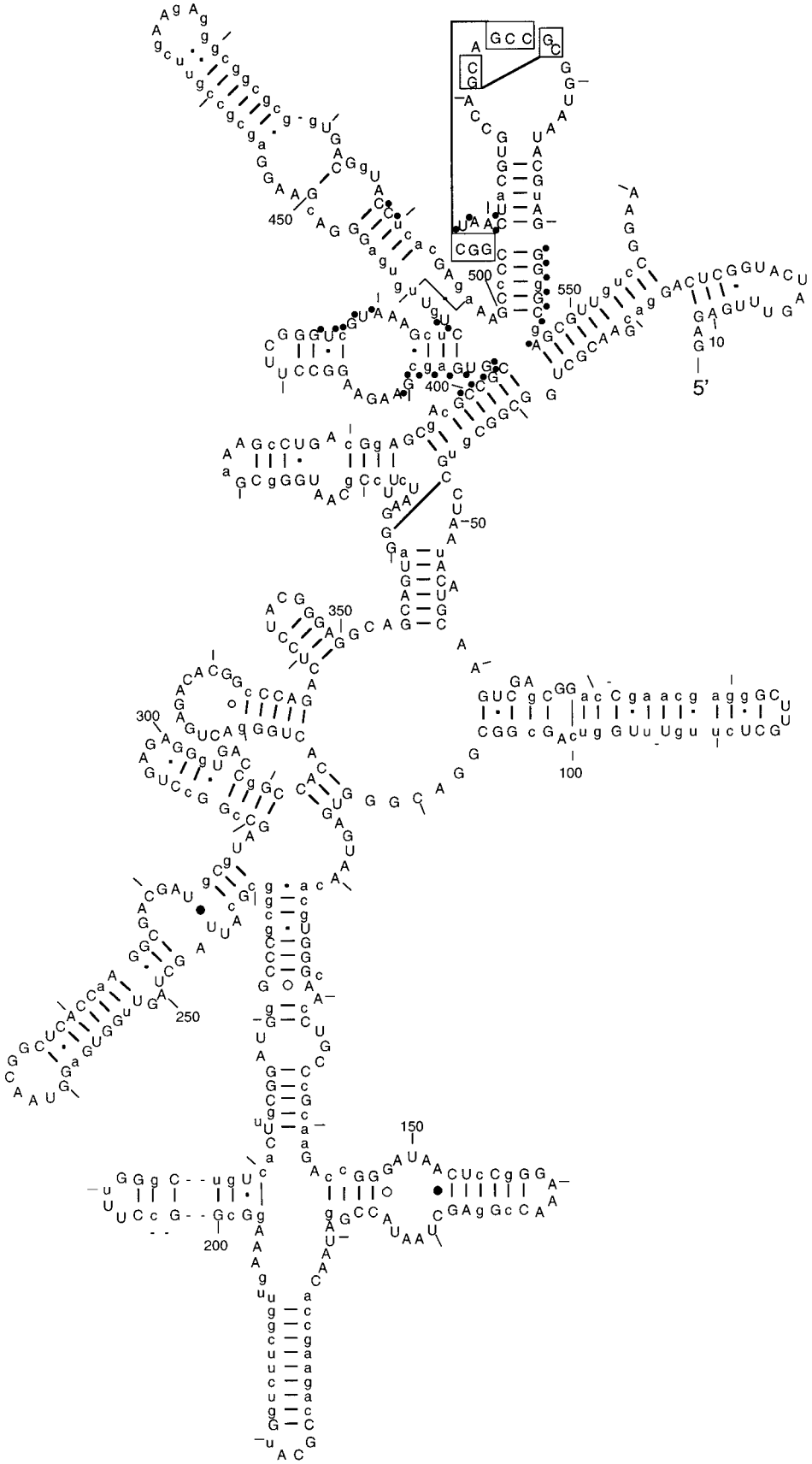

FIGURE 1: The 5′ domain of Bst 16S rRNA. The sequence has been superimposed on a diagram of the *E. coli* secondary structure (*47*); differences from the *E. coli* sequence are depicted as lowercase letters (substitutions and insertions) or dashes (deletions). The *E. coli* numbering system has been retained for reference. Dots between nucleotides indicate the positions of phosphate oxygens that are within 3.5 Å of S4 side chains in the *Thermus thermophilus* 30S subunit structure (*10*).

MATERIALS AND METHODS

RNA Transcription. Unlabeled and ^{35}S-labeled RNAs were transcribed from linearized plasmid DNA using T7 RNA polymerase (*22*). A plasmid for transcription of the Bst 5′ domain was prepared by PCR of Bst genomic DNA. One primer contained an *Eco*RI restriction site followed by the T7 promoter sequence and 19 nucleotides corresponding to the sequence at or near the 5′ end of Bst 16S rRNA (*23*, *24*); the other primer was complementary to nucleotides 544−560 of the Bst 16S rRNA gene (*E. coli* numbering) and contained a *Bam*HI restriction site. The PCR product was cloned into pUC18 cut with *Eco*RI and *Bam*HI to give pAEW33. The DNA sequence of the cloned fragment exhibited a number of differences from the published sequence (three deletions, six insertions, and five substitutions) (*24*); all the differences are consistent with the expected bacterial rRNA secondary structure (Figure 1). Runoff transcription of *Bam*HI-cut pAEW33 gives an RNA with a 5′ G and a 3′ GGAUC sequence in addition to 565 nt of Bst rRNA. This transcript is termed "16S 5′ domain RNA". Transcription of the homologous sequence from *E. coli* 16S rRNA has been described (*15*). pTRS2 transcribes a 505 nt fragment of *E. coli* 23S rRNA when cut with *Sal*I (*25*). Mixtures for labeled transcription reactions contained 25 μCi of [α-^{35}S]ATP (NEN Dupont or Amersham). RNA was purified with reverse phase NENsorb purification cartridges (NEN Dupont), resuspended in TE [10 mM Tris (pH 7.5) and 1 mM EDTA], and stored at −20 °C for up to 3 weeks.

Purification of S4 Proteins. A plasmid containing the Bst S4 gene has been described (*20*); the gene was recloned into pET 11a (*26*) and transformed into BL21(DE3) cells. One liter of LB medium containing 50 mg of ampicillin was innoculated with 10 mL of overnight cell culture. Cells were grown to an OD_{600} of 0.6 before inducing with 1 mM isopropyl β-D-thiogalactopyranoside (IPTG). Cells were pelleted and resuspended in buffer containing 20 mM MES (pH 5.5), 0.5 M KCl, 2 M urea, 1 mM phenylmethanesulfonyl fluoride, 1 mM benzamidine, 1 mM 1-chloro-3-(tosylamido)-7-amino-L-2-heptanone, 5 mM EDTA, and 10 μg/mL DNase. They were lysed by twice being passed through a French pressure cell. Cell debris was removed by centrifugation at 10 000 rpm for 1 h followed by ultracentrifugation (Beckman Ti55 rotor at 45 000 rpm for 3 h) at 15 °C to remove ribosomes. The crude protein was then loaded onto an HPLC cation exchange column (Bio-Rad TSK SP5 PW), and S4 was eluted with a 0 to 1 M gradient of KCl in the same buffer that was used for lysis. Bst S4 eluted at 0.75 M KCl under these conditions. The purified protein was quantitated using a calculated extinction coefficient of 18 490 M^{-1} cm^{-1} (*27*) and was stored as 100 μM aliquots in buffer containing 30 mM Tris (pH 7.5) and 0.35 M KCl (TK buffer). The *E. coli* S4 homologue was overexpressed and purified as described previously (*15*).

Binding Constant Measurements from Filter Binding Assays. S4−RNA association constants were determined by a filter retention assay (*28*). Dilutions of S4 (in TK buffer) were made in siliconized 1.5 mL tubes (Ambion) at concentrations ranging from 10^{-12} to 10^{-5} M, and kept at 4 °C until they were needed. ^{35}S-labeled RNA was diluted with TK buffer containing 20 mM $MgCl_2$. Under standard assay conditions, RNA was added to each protein aliquot at 4 °C so that the final buffer contained TK buffer in addition to 8 mM $MgCl_2$ (TKM_8), and $\sim 10^4$ cpm of RNA in a 60 μL volume. The mixture was incubated at 42 °C for 10 min and then cooled on ice for 5 min before filtration. In some assays, the protein was incubated at 37 °C for 20−30 min and the RNA was incubated separately at 42 °C in TKM_{20} buffer for 20 min; the protein and RNA were then placed on ice before mixing. Protein−RNA mixtures (50 μL) were filtered through 25 mm nitrocellulose filters (Schleicher and Schuell BA85) that had been soaked and degassed in TKM_8 buffer. Suction was applied to the filters with a vacuum pump for 8 s at ~15 psi (50 kPa). The filters were washed with 0.5 mL of TKM_8 buffer. Suction was applied for an additional 8 s before the filters were removed, dried, and counted by scintillation. Samples containing RNA only were filtered to determine the background level of retention of RNA, and aliquots of RNA alone were spotted and dried onto filters for a measure of the total amount of RNA.

Data were normalized to the total amount of RNA contained in each assay, and fit to a binding isotherm that assumes two proteins bind independently to two different RNA sites with different association constants (K_1 and K_2) and different filter retention efficiencies (ϵ_1 and ϵ_2). The binding polynomial describing all the possible states of the RNA is $P = 1 + K_1[S4] + K_2[S4] + K_1K_2[S4]^2$, and the fraction of the RNA retained on the filter is

$$\frac{[RNA]_{bd}}{[RNA]_0} = B + [\epsilon_1 K_1[S4] + \epsilon_2 K_2[S4] + (\epsilon_1 + \epsilon_2 - \epsilon_1\epsilon_2)K_1K_2[S4]^2]P^{-1} \quad (1)$$

B is the background level of retention of RNA in the absence of protein. The term for the retention efficiency of the $S4_2$−RNA complex assumes that the probability of the complex being retained by one protein is independent of the presence of the other protein; i.e., the probability of passing through the membrane is $(1 - \epsilon_1)(1 - \epsilon_2)$ (*29*). Since the concentration of labeled RNA in these assays was $\sim 10^{-10}$ M, the concentration of complexes was always small compared to the total protein concentration, and the total S4 concentration could be used for the free S4 concentration in the above equation. In the experiments reported here, the variation between independently determined binding constants was typically less than ~30%.

In some titrations, unlabeled RNA was added so that the S4:RNA stoichiometry of the complexes could be measured. Filter binding curves were calculated by the same approach described above, assuming either *n* independent binding sites in the case of a 23S rRNA fragment [$P = (1 + K[S4])^n$] or, for binding to the 16S 5′ domain RNA, two classes of tight and weak sites with different numbers of each [$P = (1 + K_1[S4])^n(1 + K_2[S4])^m$]. Retention efficiencies were assumed to be the same for all equivalent sites, but different for tight and weak sites. As in eq 1, retention of a complex with *n* bound proteins is related to the independent probabilities of any one of the proteins binding the filter; i.e., in the case of a complex with three proteins, the overall retention is $1 - (1 - \epsilon_1)(1 - \epsilon_2)(1 - \epsilon_3)$.

RESULTS

Strong and Weak S4−rRNA Complexes. The first equilibrium measurements of the affinity of *E. coli* S4 for 16S

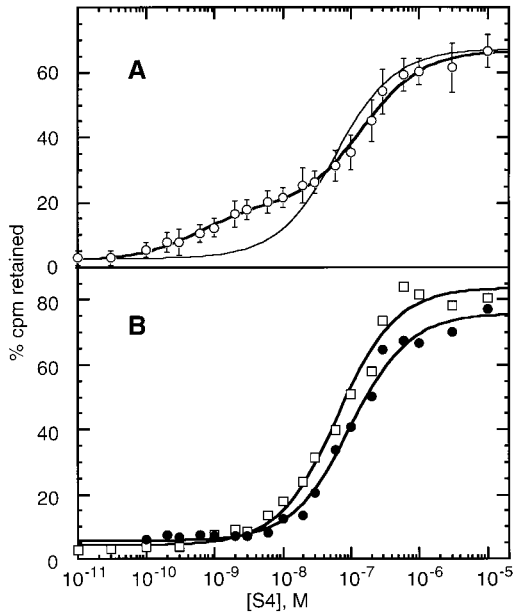

FIGURE 2: Filter assays of Bst S4 binding to 16S and 23S rRNA fragments in TKM_8 buffer. (A) Bst 5′ domain RNA complexes formed at 42 °C ($K_1 = 1.7$ nM^{-1}, $E_1 = 0.171$; $K_2 = 6.5$ μM^{-1}, $E_2 = 0.575$; $B = 0.026$). Points from 12 data sets have been averaged together; approximate errors in the measurements are represented by the error bars. Estimated errors for the binding constant measurements are ±30% for K_1 and ±12% for K_2. For comparison, the fit to the 4 °C titration in panel B is also shown (thin line), normalized to the same maximum retention as the 42 °C curve. (B) (□) Titration of Bst 5′ domain RNA complexes formed at 4 °C ($K = 16$ μM^{-1}, $E = 0.84$, $B = 0.043$). Points are the averages of five data sets. (●) Titration of a 505 nt fragment of *E. coli* 23S RNA ($K_a = 9.9$ μM^{-1}, $E = 0.76$, $B = 0.060$). Points are the averages of five data sets.

rRNA were achieved using filter binding assays in which protein−RNA complexes passed through the filter while the free protein was retained (*12*, *30*); evidently, the large rRNA prevented bound S4 from interacting with the filter. Those studies reported unit binding stoichiometry and an affinity of 18 μM^{-1} under standard ribosome reconstitution conditions (buffer containing 0.29 M KCl and 20 mM $MgCl_2$; see ref *31*). When rRNA fragments of <900 nt were used, S4 complexes were retained on filters (*13*). RNA fragments containing nucleotides 39−500 of the 16S rRNA bound with affinities of ∼15 μM^{-1} at KCl and $MgCl_2$ concentrations similar to those in the ribosome reconstitution buffer (*13*).

Via application of the filter binding assay to the Bst 5′ domain fragment of 16S RNA (corresponding to *E. coli* nucleotides 7−560; Figure 1), apparent binding constants for Bst S4 similar to those of the *E. coli* S4−16S RNA complex were measured (Figure 2B). In these assays, protein and RNA were renatured separately and then cooled on ice before forming the complex (see Materials and Methods). When RNA and protein were instead heated together at 42 °C for 10 min, a biphasic curve was obtained (Figure 2A). This curve was fit to a binding isotherm that assumes formation of two stoichiometric protein−RNA complexes with different affinities and filter retention efficiencies (see Materials and Methods; the assumption of unit stoichiometry is tested below). The two apparent affinities, 1.7 nM^{-1} and 6.5 μM^{-1}, differ by more than 100-fold.

The tight binding portion of the biphasic S4 binding curves has a rather low retention efficiency, ∼20% (Figure 2A). After sample is applied to filters, an additional aliquot of buffer is run through the filter to reduce the background level of protein-independent RNA binding. To see if this wash step was removing complexes from the filter, the aliquot of buffer was varied in volume (from 0.5 to 3 mL), temperature (4 °C or room temperature), and salt concentration (up to 0.6 M KCl). Neither the tight or weak portions of the binding curves were affected by these variations. Omission of the wash step increased the background level of retention of the RNA and the variability of the data without increasing the retention efficiency. Inclusion of 50 μg/mL BSA, which can prevent nonspecific protein adsorption on surfaces, also did not affect the binding curve. We conclude that low retention efficiency is an intrinsic property of the tight complex and not an artifact of complex dissociation from the filter.

Nonspecific S4 Binding to 23S rRNA. To assess the level of nonspecific binding for Bst S4, we used a fragment of 23S rRNA (505 nt) that was roughly the same size as the 5′ domain of 16S rRNA (558 nt) used in the filter binding assay (Figure 2B). The apparent binding affinity is 9.9 μM^{-1} and the filter retention efficiency ∼65%, both comparable to the weak binding observed with 5′ domain RNA. (This calculation of the binding constant assumes a stoichiometry of one protein per RNA, and overestimates the actual affinity; see the determination of stoichiometry below.) With a smaller, 103 nt fragment of 23S rRNA and Bst S4, the apparent binding constant was reduced 2-fold with no change in retention efficiency (data not shown).

Binding Stoichiometry. Filter binding assays typically use low concentrations of labeled RNA and excess protein so that the concentration of the complex is negligible compared to the total concentration of added protein. Fitting such data to a binding isotherm determines the product *nK*, where *n* is the number of binding sites and must be determined in a separate experiment. We supposed that tight binding of S4 to the 16S rRNA 5′ domain might represent a specific, stoichiometric complex and that the weak binding would reflect S4 binding at additional, nonspecific sites. Therefore, S4 binding stoichiometries were determined in both tight and weak parts of the biphasic curve, by adding unlabeled RNA to the binding reaction in concentrations comparable to or larger than the expected dissociation constant of the complex. The additional RNA increases the amount of protein needed to reach a given saturation level, and the binding stoichiometry can be calculated from the increase.

Figure 3A shows the result when S4 titrated 5 nM 5′ domain RNA under tight binding conditions. The binding curve has been shifted to higher S4 concentrations in the initial part of the titration, compared to the analogous curve with only labeled RNA present (dotted line in Figure 3A), though the low concentration of added RNA has a negligible effect on the curve at higher S4 levels. Simulations of expected binding curves were made assuming either one or two tight binding sites and a single weak site, and using the value of *nK* calcuated from Figure 2 data (i.e., $n = 1$ and $K = 1.7$ nM^{-1}, or $n = 2$ and $K = 0.85$ nM^{-1}). It is clear that the tight binding complex has the approximately 1:1 stoichiometry expected for a specific interaction; this experiment also indicates that the protein is fully active in binding. (Deviations from the calculated curve when >1 equiv of S4 has been added could be a result of assumptions made about the weak binding.) To examine the weak binding portion of

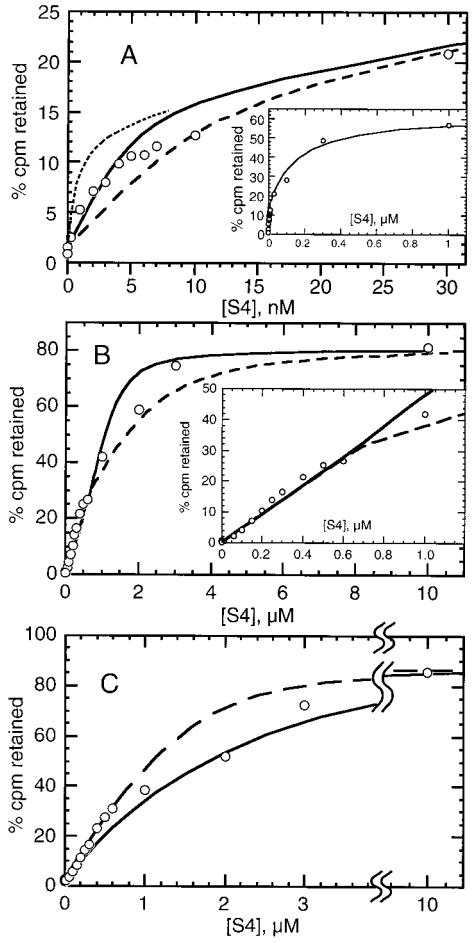

FIGURE 3: Stoichiometry of S4−rRNA complexes. (A) S4 titration of 5 nM 16S 5′ domain RNA under tight binding conditions. Curves are calculated using tight and weak binding affinities from Figure 2 and either one [(—) $E_1 = 0.14$, $E_2 = 0.55$] or two [(- - -) $E_1 = 0.075$, $E_2 = 0.50$] tight binding sites per RNA; see text for further details. To show the effect of adding unlabeled RNA to the titration, the dotted line is calculated using the same parameters that were used for the single-binding site curve, but assuming that only a trace amount of RNA is present (as in Figure 2). The panel and inset show the same data set and curves, but with different S4 concentration scales. Panel B is the same as panel A, but with 0.7 μM RNA. Binding curves are calculated using binding affinities from Figure 2, with one strong binding site ($E_1 = 0.14$) and either one [(—) $E_2 = 0.72$] or two [(- - -) $E_2 = 0.50$] weak binding sites per RNA. (C) S4 titration of 1 μM 505 nt 23S rRNA fragment. Binding curves are calculated using binding affinities from Figure 2 and two [(- - -) $E_2 = 0.72$] or three [(—) $E_2 = 0.58$] equivalent sites.

the biphasic curve, other titrations included 0.7 μM 5′ domain RNA (Figure 3B). Curves calculated using values of *nK* from data in Figure 2 suggest that than one or two weak binding sites are present in addition to the one strong binding site. Presumably the weak binding represents nonspecific interactions.

The stoichiometry of complexes formed with a 23S rRNA fragment was also measured, with 1 μM RNA fragment added to each assay point. The titration data, shown in Figure 3C, are bracketed by curves calculated assuming either two or three independent binding sites per RNA and the value of *nK* derived from titrations in the absence of unlabeled RNA (Figure 2). The stoichiometry and affinity are similar to those estimated for the weak binding part of the 16S rRNA 5′ domain RNA. We conclude that S4 has a relatively high

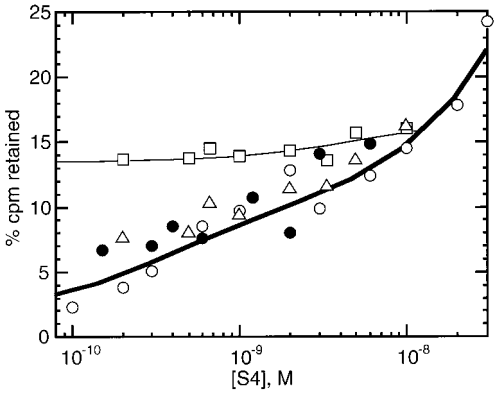

FIGURE 4: Equilibrium formation of tight S4−RNA complexes. Complexes were formed in TKM_8 buffer at 42 °C and a protein concentration of 10 nM, diluted with various amounts of TKM_8 buffer at 4 (□), 22 (△), or 42 °C (●), and incubated for an additional 10 min at the chosen temperature. A binding data set without the additional incubation is shown for comparison (○), and the thick solid line has been fit to these data by the same method used to draw in Figure 2.

nonspecific binding affinity (~3−5 μM^{-1}) under these buffer conditions, but that a large RNA cannot accommodate more than one S4 for every ~200 nt.

Tight Binding Complexes Are in Equilibrium. To be sure that the tight binding complexes were in equilibrium with the free protein, Bst S4−5′ domain complexes were formed at 42 °C, diluted 2−50-fold, and further incubated at the same temperature (see Materials and Methods). If the complexes were in equilibrium with the free protein, dilution would cause partial dissociation to the new equilibrium level. Figure 4 shows that retention of diluted complexes essentially retraced the original binding curve. As the change in signal (RNA retention) was small in these experiments, data tended to be variable; the figure shows a typical data set with minor deviations from a normal binding curve. The deviations were not systematic between the data sets and did not suggest any deviation from equilibrium behavior.

The same experiment was also carried out with continued incubation at 4 or 22 °C after dilution. A temperature of 22 °C produced the approximately same results as obtained at 42 °C. However, at 4 °C, even 50-fold dilution does not diminish the level of retention of complexes (Figure 4). Thus, S4 becomes kinetically trapped on the RNA at low temperatures.

Temperature Dependence of Tight Complex Formation. The range of temperatures over which tight complexes could be formed was explored. S4−RNA complexes were routinely mixed on ice, heated to the temperature of interest, and then cooled on ice before filtering; similar results were obtained if the initial or final temperatures were increased to 22 °C (data not shown). However, incubation at temperatures between 35 and 50 °C was required to observe tight complexes; higher or lower temperatures considerably reduced the extent of complex formation (Figure 5). Fitted values of the tight binding constant vary only ~3-fold over the 22−50 °C temperature range; thus, the binding affinity is not strongly temperature dependent.

We also attempted to observe the kinetics of complex formation at various temperatures. When protein and RNA were mixed at 42 °C, binding was complete within 1 min (Figure 6). Only at 30 °C was complex formation slowed to

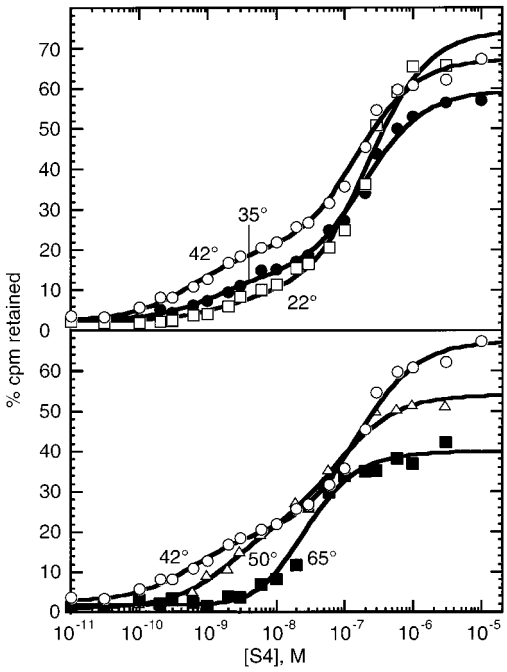

FIGURE 5: Effect of incubation temperature on Bst S4−RNA complex formation in TKM_8 buffer. Protein and 16S 5′ domain RNA were incubated together for 10 min at 22 (□), 35 (●), 42 (○), 50 (△), or 65 °C (■). The same 42 °C data set has been duplicated in both panels for comparison. The 65 °C data have been fit to a single-site binding isotherm; the other curves were fit to the two-site model described in Materials and Methods. K_1 and ϵ_1 are 0.793 nM^{-1} and 0.137, 1.73 nM^{-1} and 0.197, and 0.481 nM^{-1} and 0.219 for the 35, 42, and 50 °C data sets, respectively. Uncertainties in K_1 are approximately ±30%.

a time scale of several minutes. Though the small signal and short time scale of the reaction preclude accurate measurement of the rate constant, we estimate a lower limit of $\sim 10^7$ M^{-1} s^{-1} at 30 °C.

Mg^{2+} and K^+ Dependences of S4−rRNA Interactions. Mg ion promotes folding of RNA into compact structures and may, as a consequence, stimulate protein binding (*32*, *33*). To see if the tight S4−rRNA complex is Mg^{2+} dependent, we first renatured 5′ domain RNA at 42 °C in buffers with Mg^{2+} concentrations as high as 40 mM; these treatments did not promote tight complex formation at 0 °C. Binding assays were then repeated with various concentrations of Mg^{2+} during co-incubation of protein and RNA at 42 °C; binding affinities of 0.11 (0.5 mM Mg^{2+}), 2.2 (2 mM Mg^{2+}), and 0.35 nM^{-1} (16 mM Mg^{2+}) were measured. (Affinities are the averages of three determinations, and have associated errors of ∼50%.) Titrations were also repeated with 1 mM EDTA substituting for Mg^{2+}. These conditions reduced tight complex formation to undetectable levels (Figure 7). We conclude that Mg^{2+} concentrations on the order of 1 mM are essential for forming a specific S4−rRNA complex (Figure 7, inset). The drop off in binding affinity at high Mg^{2+} concentrations can be attributed to the effectiveness of Mg^{2+} as a competitor for electrostatic interactions between protein and nucleic acids.

The sensitivity of S4−RNA complexes to K^+ concentrations was also examined (Figure 8). Both tight and weak portions of the binding curve shifted to higher protein concentrations (lower affinity) as the salt concentration was increased (Figure 8A). Doubling the KCl concentration

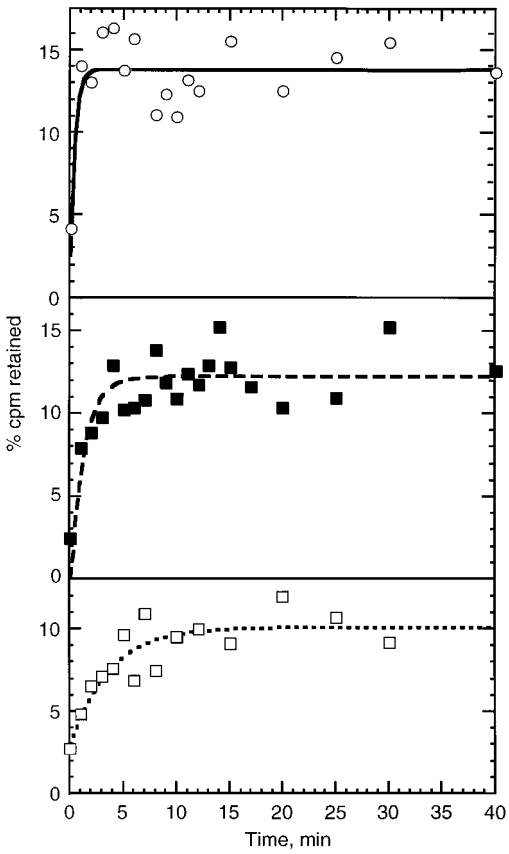

FIGURE 6: Kinetics of Bst S4−rRNA binding in TKM_8 buffer, using 1 nM protein. Complexes were formed at 42 [top (○)], 35 [middle (■)], or 30 °C [bottom (□)], and data sets were fit to a first-order exponential with time constants of 2.4, 0.77, and 0.31 min^{-1}, respectively.

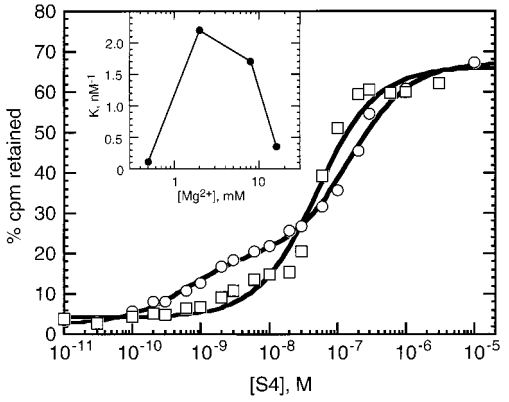

FIGURE 7: Mg^{2+} requirement for Bst S4−rRNA binding. Binding assays were carried out under standard conditions in either TKM_8 buffer (○) or TK buffer with 1 mM EDTA (□). The inset shows tight Bst S4−5′ domain RNA binding affinity as a function of Mg^{2+} concentration. Binding assays were carried out under standard conditions, but with various Mg^{2+} concentrations.

weakened the tight complex affinity by more than 2 orders of magnitude, while there was a smaller decrease in the weak binding affinity. The binding constants extracted from these titration curves are plotted in Figure 8B; $-\partial[\log(K)]/\partial(\log[K^+])$ is 9.3 for tight binding and 6.3 for weak binding.

Comparison with E. coli S4. Previous studies of Eco S4 reported similar binding constants whether protein and RNA were heated together under ribosome reconstitution conditions (*12*) or mixed at low temperatures (*13*). Thus, the Eco S4−RNA complex is qualitatively different from the Bst

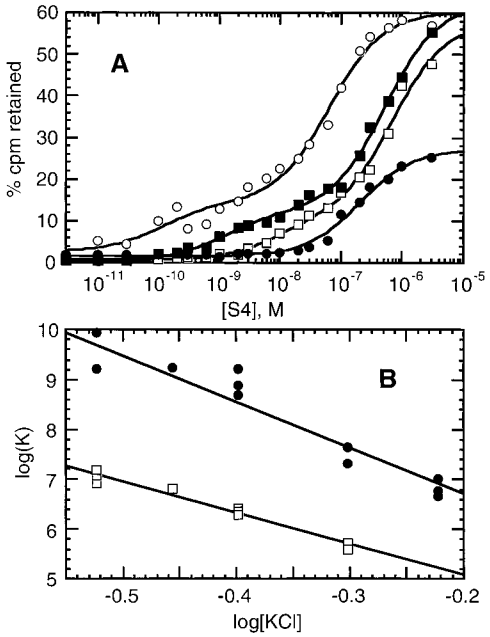

FIGURE 8: Salt dependence of Bst S4−RNA binding. (A) Binding curves obtained under standard conditions but with various KCl concentrations: 300 (○), 400 (■), 500 (□), and 600 mM (●). Curves are best fits using two binding constants, with the exception of the 600 mM data set, which was fit with a single K. (B) Plot of $\log(K_a)$ vs log[KCl] for either high-affinity binding (●) or weak binding (□). Lines are linear least-squares fits to the data, with slopes and intercepts of −9.3 and 4.9 (tight binding) or −6.3 and 3.8 (weak binding), respectively.

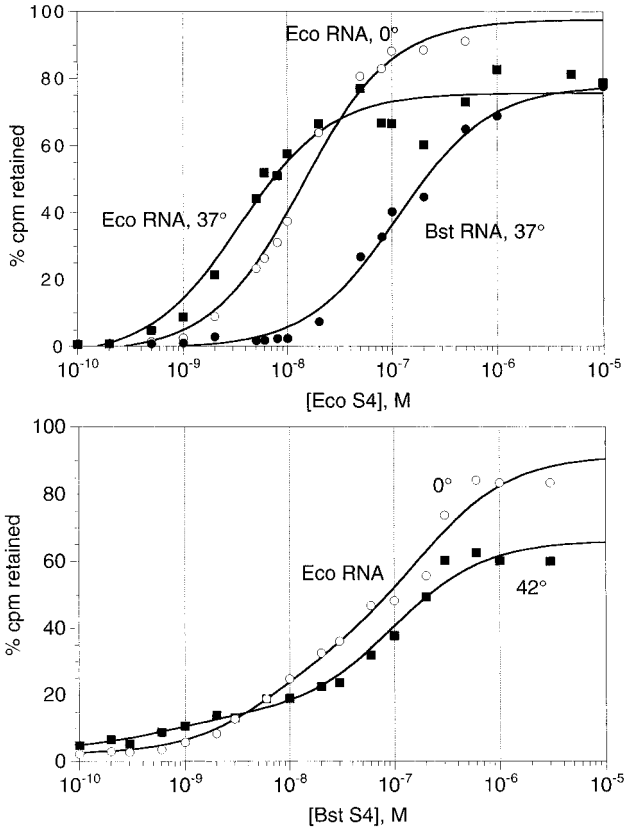

FIGURE 9: Heterologous binding between Eco and Bst S4 and 5′ domain RNAs. (A) Eco S4 binding to 5′ domain RNAs in TKM_8 buffer: (■) protein and Eco RNA warmed together at 37 °C for 10 min before filtering (284 μM^{-1}), (○) protein and Eco RNA mixed and incubated at 0 °C (K = 7.2 μM^{-1}), and (●) protein and Bst RNA warmed together at 37 °C for 10 min before filtering (K = 8.8 μM^{-1}). Binding curves are least-squares fits of single-site isotherms. (B) Bst S4 binding Eco 5′ domain RNA in TKM_8 buffer: (■) protein and RNA warmed together at 42 °C for 10 min before filtering (K_1 = 1.5 nM^{-1}, K_2 = 0.01 nM^{-1}) and (○) protein and RNA mixed and incubated at 0 °C (K_1 = 1.5 μM^{-1}, K_2 = 5.5 μM^{-1}). Binding curves are fits to the two-site model described in Materials and Methods.

complex, in being kinetically competent to form a specific complex at low temperatures. To confirm this difference, we repeated binding assays under our standard conditions with the homologous Eco S4 and 5′ domain RNA (Figure 9A). As in previous filter binding studies (*13*), the Eco S4 protein exhibited a single binding phase with high retention efficiency, and inclusion of a 37 °C incubation increased the binding affinity by no more than 4-fold, to 280 μM^{-1} (Figure 9A). This affinity is higher than that reported previously but still significantly lower than that of the Bst S4−RNA complex, and the lack of a requirement for a heat activation step is confirmed.

To determine whether the different behavior of the Eco and Bst complexes at low temperatures is a property of the protein, the RNA, or both, we also examined the heterologous complexes. Eco S4 binding to Bst 5′ domain RNA did not show any indication of a tight complex (Figure 9A). In contrast, Bst S4 binding to Eco 5′ domain RNA was very similar to its interaction with Bst RNA; i.e., incubation at 42 °C results in the appearance of a tight complex with an affinity of $\sim 10^9$ M^{-1} (Figure 9B). The binding curve created with only low-temperature incubation does show some systematic deviation from a single-binding site isotherm and is better fit by a two-site binding isotherm. However, the requirement for a heat activation step seems to be largely a function of the protein.

DISCUSSION

Structure of the S4−rRNA Complex. The crystal structure of the entire 30S ribosomal subunit from *Thermus thermophilus* has been determined recently (*9*, *10*). The Bst S4 and 16S 5′ domain rRNA sequences are closely homologous to those from *T. thermophilus*, and the structure of the globular domains of S4 within the *T. thermophilus* ribosome is not significantly different from the structures determined for free Bst S4 (*18*−*20*). [The S4 N-terminal sequence is disordered in the absence of RNA (*21*), but adopts a specific conformation in the ribosome.] The S4−rRNA contact surface in the *T. thermophilus* crystals is undoubtedly very similar to the homologous Bst complex, and several features of the surface help in the interpretation of the thermodynamic results discussed in the following sections.

As suggested by footprinting experiments with Eco S4 (*7*, *8*), the protein straddles the junction of five helices located in the "upper" half of the 5′ domain, as drawn in Figure 1. The contacts are numerous and predominantly made with the backbone; thus, nonbridging phosphate oxygens of 31 nucleotides are close (≤3.5 Å) to protein side chains (Figure 1), while only seven bases are hydrogen bonded to S4. Fifteen of the side chains approaching phosphates are arginine and lysine residues. Not all of these positions are conserved as basic residues in Bst S4, but the total number is likely to be very similar. Last, the contacted backbone phosphates are largely in the approximate A-form helical conformation.

The five helices of the recognized junction region are closely packed together, yet have relatively few sets of tertiary contacts that would maintain their orientation in the absence of S4. It therefore seems plausible that the junction region is poorly structured in naked RNA and that S4 binding promotes the helix arrangement seen in the intact ribosome. Among the few hydrogen bonds made by S4 to RNA bases is a set of highly conserved contacts with two stacked base pairs from different helices [C436-G406 and U437-A496 (*E. coli* rRNA numbering), bonding to His123 and Gln119 (*T. thermophilus* numbering)]. This feature of the complex also hints that a function of S4 in ribosome assembly is to stabilize coaxial stacking of two helices within the five-helix junction.

Specific and Nonspecific Binding of S4 to 16S rRNA. Recognition of ribosomal RNA by primary binding proteins typically takes place with affinities on the order of 10^6-10^8 M^{-1} in the high-salt buffers used for ribosome reconstitution (*30*, *34*), and previous work with *E. coli* S4 had placed its binding constant in the middle of this range ($\sim 2 \times 10^7$ M^{-1}; *12*, *13*). (Much tighter binding constants have been reported for some ribosomal proteins in buffers containing lower salt concentrations; cf. refs *33* and *35*.) Thus, observing such a high affinity, ~ 1 nM^{-1}, for Bst S4 binding its cognate 5′ domain RNA was unexpected. A nanomolar S4−rRNA dissociation constant is probably not essential for ribosome assembly, as the concentration of free S4 in the cell is substantially higher (~ 1 μM; *36*), and additional S4−protein and protein−RNA interactions stabilize the S4−RNA complex in the assembled subunit. However, the high affinity is consistent with the unusually large number of protein−RNA contacts, which might be needed for S4 to manipulate the rRNA five-helix junction into a functional conformation.

A nonspecific binding mode of Bst S4 also has an unusually high binding affinity, on the order of 10^6-10^7 M^{-1} (in ribosome reconstitution buffer) and comparable to that of many specific protein−RNA complexes. Two factors may contribute to this promiscuous behavior: (i) much of the S4−RNA interface is roughly A-form helical backbone, which will be commonly found in structured RNAs, and (ii) the disordered N-terminal region is very basic in Bst S4 (eight Arg and Lys residues, and only one Glu) and may be adaptable to many RNAs. The N-terminal sequence is, however, essential for specific, high-affinity binding to ribosomal RNA (R. B. Gerstner and D. E. Draper, unpublished observations).

The steep salt dependence of S4−rRNA binding is notable, as the value of $-\partial[\log(K)]/\partial(\log[KCl])$ for this interaction (9.3) is larger than those observed for other ribosomal protein−RNA complexes [1.3 for L11 and 4.8 for S8 (*35*, *37*)]. The salt dependence of basic peptides binding polynucleotides is proportional to the number of basic residues in the peptide (*38*), but this simple relationship does not extend to specific protein−RNA complexes (*37*); other factors, such as protein or RNA conformational changes and anion binding by protein, may also affect the salt dependence. Nevertheless, the extensive protein contacts with backbone phosphates and the large number of S4 basic residues contacting phosphates [15 in the *T. thermophilus* 30S subunit crystal structure (*10*) and probably a comparable number in Bst S4] are consistent with the steep salt dependence of binding. Nonspecific binding is less steeply salt dependent than specific binding; thus, binding becomes more specific at lower salt concentrations. This is opposite from the usual case with DNA−protein interactions. The nonspecific binding of Lac repressor, for instance, is almost all attributable to salt-dependent, electrostatic interactions with the DNA backbone (*39*). Specific binding to the DNA operator is much less steeply salt dependent, and specificity derives from a large, salt-independent free energy of interaction with bases (*40*, *41*).

A last comment concerning S4 binding specificity is the role of Mg ion, which, at low concentrations, promotes formation of specific complexes but is not needed for nonspecific binding. Mg^{2+} strongly stabilizes compact RNA folds relative to less tightly folded structures, simply by virtue of its preferential interactions with the higher charge density of a compact RNA (*42*). Chelation of dehydrated ions by RNA tertiary structures may add to the stabilization of folded RNAs as well (*43*). Thus, the linkage of S4−RNA complex formation to an uptake of Mg ions implies that the protein imposes a more compact conformation on the RNA, in line with suggestions that S4 organizes the RNA for subsequent protein binding during subunit assembly.

Temperature Dependence of S4−RNA Complex Formation. E. coli S4 binds specifically to 16S 5′ domain RNA at cold temperatures, as shown in this study, a previous binding study (*13*), and 30S subunit reconstitution studies (*3*, *44*). The very steep temperature dependence of Bst S4 binding to 16S 5′ domain RNA was therefore unexpected, and we initially attributed this different behavior to inappropriate structures in Bst RNA. The kinetics of large RNA folding may be strongly temperature dependent, because of the activation energy needed to escape stable but incorrectly folded structures (*45*, *46*). We reasoned that ribosomal RNAs may strongly depend on proteins to fold properly, and thus be particularly prone to folding into inappropriate (and slowly exchanging) structures at low temperatures. However, our data point to the Bst S4 protein as the source of temperature-dependent binding. Comparison of Bst and Eco S4 binding Eco RNA at low and high temperatures shows that Eco S4 binding is relatively insensitive to temperature, while Bst S4 requires higher temperatures for specific binding (Figure 9). Thus, Eco RNA is competent to bind protein at low temperatures, and we conclude that higher temperature is needed to activate the Bst S4 protein.

What aspect of the binding reaction might be temperature dependent? One possibility is that the protein undergoes a reversible, temperature-dependent conformational change that favors binding at high temperatures. We have no data to support this possibility, but cannot rule it out. A more interesting possibility is that the N-terminus of the protein, which is disordered in solution and highly basic, first binds nonspecifically to RNA, where it has a large activation energy for rearrangement to the correctly folded form. The N-terminal domain sequence differs considerably between the Eco and Bst proteins, which might explain the difference in binding behavior between the two proteins.

ACKNOWLEDGMENT

We thank Anja Wade for cloning the Bst 5′ domain RNA sequence.

REFERENCES

1. Zimmermann, R. A., Muto, A., Fellner, P., Ehresmann, C., and Branlant, C. (1972) *Proc. Natl. Acad. Sci. U.S.A. 69*, 1282−1286.
2. Nomura, M. (1973) *Science 179*, 864−873.
3. Held, W. A., and Nomura, M. (1973) *Biochemistry 12*, 3273−3281.
4. Nowotny, V., and Nierhaus, K. H. (1988) *Biochemistry 27*, 7051−7055.
5. Ehresmann, C., Stiegler, P., Carbon, P., Ungewickell, E., and Garrett, R. A. (1980) *Eur. J. Biochem. 103*, 439−446.
6. Mackie, G. A., and Zimmermann, R. A. (1978) *J. Mol. Biol. 121*, 17−39.
7. Stern, S., Wilson, R. C., and Noller, H. F. (1986) *J. Mol. Biol. 192*, 101−110.
8. Powers, T., and Noller, H. F. (1995) *RNA 1*, 194−209.
9. Schluenzen, F., Tocilj, A., Zarivach, R., Harms, J., Gluehmann, M., Janell, D., Bashan, A., Bartels, H., Agmon, I., Franceschi, F., and Yonath, A. (2000) *Cell 102*, 615−623.
10. Wimberly, B. T., Brodersen, D. E., Clemons, W. M., Jr., Morgan-Warren, R. J., Carter, A. P., Vonrhein, C., Hartsch, T., and Ramakrishnan, V. (2000) *Nature 407*, 327−339.
11. Powers, T., and Noller, H. F. (1995) *J. Biol. Chem. 270*, 1238−1242.
12. Schwarzbauer, J., and Craven, G. R. (1981) *Nucleic Acids Res. 9*, 2223−2237.
13. Vartikar, J. V., and Draper, D. E. (1989) *J. Mol. Biol. 209*, 221−234.
14. Sapag, A., Vartikar, J. V., and Draper, D. E. (1990) *Biochim. Biophys. Acta 1050*, 34−37.
15. Baker, A. M., and Draper, D. E. (1995) *J. Biol. Chem. 270*, 22939−22945.
16. Nomura, M., Traub, P., and Bechmann, H. (1968) *Nature 219*, 793−799.
17. Held, W. A., Gette, W. R., and Nomura, M. (1974) *Biochemistry 13*, 2115−2122.
18. Markus, M. A., Gerstner, R. B., Draper, D. E., and Torchia, D. A. (1998) *EMBO J. 17*, 4559−4571.
19. Markus, M. A., Gerstner, R. B., Draper, D. E., and Torchia, D. A. (1999) *J. Mol. Biol. 292*, 375−387.
20. Davies, C., Gerstner, R. B., Draper, D. E., Ramakrishnan, V., and White, S. W. (1998) *EMBO J. 17*, 4545−4558.
21. Sayers, E. W., Gerstner, R. B., Draper, D. E., and Torchia, D. A. (2000) *Biochemistry 39*, 13602−13613.
22. Draper, D. E., White, S. A., and Kean, J. M. (1988) *Methods Enzymol. 164*, 221−237.
23. Ash, C., Farrow, J. A. E., Wallbanks, S., and Collins, M. D. (1991) *Lett. Appl. Microbiol. 13*, 202−206.
24. Fox, G. E., and Rossler, D. (1991) *Syst. Appl. Microbiol. 14*, 266−269.
25. Ryan, P. C., and Draper, D. E. (1989) *Biochemistry 28*, 9949−9956.
26. Studier, F. W., Rosenberg, A. H., Dunn, J. J., and Dubendorff, J. W. (1990) *Methods Enzymol. 185*, 60−89.
27. Gill, S. C., and von Hippel, P. H. (1989) *Anal. Biochem. 182*, 319−326.
28. Draper, D. E., Deckman, I. C., and Vartikar, J. V. (1988) *Methods Enzymol. 164*, 203−220.
29. Woodbury, C. P., Jr., and von Hippel, P. H. (1983) *Biochemistry 22*, 4730−4737.
30. Spicer, E., Schwarzbauer, J., and Craven, G. R. (1977) *Nucleic Acids Res. 4*, 491−499.
31. Traub, P., Mizushima, S., Lowry, C. V., and Nomura, M. (1971) *Methods Enzymol. 20*, 391−407.
32. Xing, Y., and Draper, D. E. (1996) *Biochemistry 35*, 1581−1588.
33. Batey, R. T., and Williamson, J. R. (1998) *RNA 4*, 984−997.
34. Spierer, P., Bogdanov, A. A., and Zimmermann, R. A. (1978) *Biochemistry 17*, 5394−5398.
35. Mougel, M., Ehresmann, B., and Ehresmann, C. (1986) *Biochemistry 25*, 2756−2765.
36. Gausing, K. (1974) *Mol. Gen. Genet. 129*, 61−75.
37. GuhaThakurta, D., and Draper, D. E. (2000) *J. Mol. Biol. 295*, 569−580.
38. Mascotti, D. P., and Lohman, T. M. (1997) *Biochemistry 36*, 7272−7279.
39. deHaseth, P. L., Lohman, T. M., and Record, M. T., Jr. (1977) *Biochemistry 16*, 4783−4790.
40. Record, M. T., deHaseth, P. L., and Lohman, T. M. (1977) *Biochemistry 16*, 4791−4796.
41. Ha, J. H., Capp, M. W., Hohenwalter, M. D., Baskerville, M., and Record, M. T., Jr. (1992) *J. Mol. Biol. 228*, 252−264.
42. Misra, V. K., and Draper, D. E. (2000) *J. Mol. Biol. 299*, 813−825.
43. Misra, V. K., and Draper, D. E. (1998) *Biopolymers 48*, 113−135.
44. Traub, P., and Nomura, M. (1969) *J. Mol. Biol. 40*, 391−413.
45. Pan, J., and Woodson, S. A. (1998) *J. Mol. Biol. 280*, 597−609.
46. Gluick, T. C., Gerstner, R. G., and Draper, D. E. (1997) *J. Mol. Biol. 270*, 451−463.
47. Gutell, R. R. (1994) *Nucleic Acids Res. 22*, 3502−3507.

BI010026I